

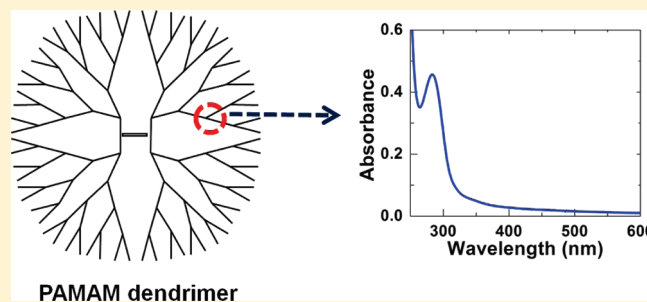
Analysis of Poly(amidoamine) Dendrimer Structure by UV–Vis Spectroscopy

Surojit Pande and Richard M. Crooks*

Department of Chemistry and Biochemistry, Texas Materials Institute, Center for Nano- and Molecular Science and Technology, The University of Texas at Austin, 1 University Station, A5300, Austin, Texas 78712-0165, United States

S Supporting Information

ABSTRACT: We report a UV–vis spectroscopic study of four different types of poly(amidoamine) dendrimers. The results indicate that the degree of protonation of the interior tertiary amines of these dendrimers correlates directly to an absorption band with λ_{max} in the range of 280–285 nm. Specifically, at low pH, the tertiary amines are protonated and the 280–285 nm band is absent. However, at elevated pH, when these groups are deprotonated, this band appears. Similar results were obtained for a simple model compound. The dependence of the 280–285 nm band on the chemical state of the tertiary amines of the dendrimers was confirmed by complexing them with Pd^{2+} and Pt^{2+} . In this case the band disappears, and it only reappears when the metal ions are decomplexed following reduction with BH_4^- . Finally, filtration experiments showed that the absorption band between 280–285 nm arises exclusively from intact, or nearly intact, dendrimers rather than low-molecular-weight fragments.



INTRODUCTION

Here we report a UV–vis spectroscopic study of poly(amidoamine) (PAMAM) dendrimers and dendrimer-encapsulated nanoparticles (DENs).^{1,2} Particular attention is focused on the origin of a prominent absorption band in the 280–285 nm region that has frequently been observed during the synthesis of DENs. Aqueous solutions of hydroxyl- and amine-terminated, fourth- and sixth-generation PAMAM dendrimers ($G_n\text{-X}$, $n = 4$ or 6, $X = \text{-OH}$ or -NH_2) also exhibit this band. We undertook this study because of concerns that this band could signal the presence of dendrimer fragments or decomposition products, which in turn could compromise the integrity of DENs.

PAMAM dendrimers have been used by our group^{1–5} and others^{6–10} as templates for the synthesis of mono- and bimetallic nanoparticles in the $\sim 1\text{--}2$ nm size range. The synthesis of DENs is generally carried out in two steps. First, a metal salt is introduced into a dendrimer-containing solution, and the resulting cations partition into the dendrimer interior. In some cases this partitioning is driven by specific interactions between the metal ions and interior functional groups,^{1,3} and in some cases by differences in solubility of the metal ions in the solvent and the dendrimer interior.^{11,12} Second, the encapsulated metal ions are chemically reduced using an appropriate reducing agent, such as BH_4^- , which results in the formation of zerovalent DENs.

UV–vis spectroscopy has proven to be a useful tool for studying both steps of the DENs synthesis. For example, the product of the first step, the metal–ion/dendrimer precursor complex, often exhibits a characteristic ligand-to-metal charge transfer (LMCT) band between 200 and 400 nm. After reduction,

the LMCT band is replaced by a broad absorbance characteristic of nanoscale metal particles.^{5,13} In addition, a band at 280–285 nm, which is associated with the reduced DENs, is also observed.¹ This same band is also apparent in aqueous solutions of G4-OH, G6-OH, G4-NH₂, and G6-NH₂ dendrimers, but at lower intensity than in solutions of DENs. Esumi and co-workers¹⁴ also reported the presence of this band when UV light was used for the synthesis of Au dendrimer-stabilized nanoparticles (DSNs).¹⁵ The same band appeared when G4-NH₂ was irradiated in the absence of a metal salt.¹⁴ Dickson and co-workers have also reported an absorption peak at 285 nm for G4-OH PAMAM dendrimers with and without encapsulated Au nanoparticles,¹⁶ and Fu and co-workers also reported that this band arises from aqueous solutions of G2 sectorial PAMAM dendrimers over the pH range 3.0–8.0.¹⁷ Finally, Bard and co-workers noted a peak at 290 nm arising from an aqueous solution of G2-OH.¹⁸ On the basis of these reports,^{1,2,14,16–18} we began the present study with the hypothesis that this band originates from interior functional groups of the dendrimer.

The structural characterization of PAMAM dendrimers and DENs has been an active area of research for some years.^{19,20} NMR spectroscopy,²¹ mass spectrometry,^{22,23} chromatography,^{24,25} quasi-elastic light scattering,²⁶ and small-angle neutron scattering²⁷ have all been applied to this problem. Three key points have emerged from these studies. First, DENs and empty PAMAM

Received: May 19, 2011

Revised: June 9, 2011

Published: June 29, 2011

dendrimers generally have the same hydrodynamic radius,^{21,26} which supports the notion of nanoparticle encapsulation. Second, PAMAM dendrimers undergo very slow decomposition when stored as solutions at room temperature.²⁸ Third, significant levels of defects are introduced into PAMAM dendrimers during their synthesis.^{22,23,25} These defects include the following: (1) dendrimer fragments produced during dendrimer synthesis and growth; (2) low-generation dendrimers initiated by incomplete removal of excess ethylenediamine (EDA) core during later-stage growth of the target; (3) skeletal defects, including the presence of missing branches inside the dendrimer; and (4) branches connected by intramolecular loops.^{22,23,25,28}

In this Article, we show that the previously unidentified absorbance peak at 280–285 nm arises from the intact dendrimer structure, and specifically from its interior tertiary amine groups, rather than from structural defects. This conclusion is supported by detailed studies of the peak intensity as a function of pH, complexation of interior tertiary amines to metal ions, and purification of the dendrimer by filtration. In addition, a model compound, which is structurally similar to dendrimeric branches, was examined and found to have spectroscopic characteristics similar to those of PAMAM dendrimers.

EXPERIMENTAL SECTION

Chemicals. G4-OH, G6-OH, G4-NH₂, and G6-NH₂ PAMAM dendrimers were purchased from Dendritech, Inc. (Midland, MI) as methanol solutions. Prior to use, the dendrimer stock solutions were dried under vacuum and then redissolved in sufficient deionized water to make a 100.0 μ M solution. K₂PdCl₄, K₂PtCl₄, NaBH₄, and 1-[bis-[3-(dimethylamino)-propyl]amino]-2-propanol were purchased from Sigma-Aldrich (Milwaukee, WI). NaOH and HCl were purchased from Fisher Scientific (Pittsburgh, PA). Aqueous solutions were prepared using 18 M Ω cm Milli-Q water (Millipore, Billerica, MA). Amicon Ultra Centrifugal Filtration devices having an Ultracel 10 kDa nominal molecular weight limit (NMWL) membrane were purchased from Millipore (Billerica, MA).

Synthesis of Pd DENs. Pd DENs were synthesized by our previously reported method.¹ Briefly, 0.20 mL of a 100.0 μ M G6-OH stock solution was diluted with 9.68 mL of water to yield a final concentration of 2.0 μ M. For G6-OH(Pd₅₅) DENs, 55 equiv of a freshly prepared 10.0 mM K₂PdCl₄ solution (0.11 mL) was added to the G6-OH solution. This mixture was allowed to stir for a minimum of 30 min to ensure complete complexation between the tertiary amines of the dendrimer and Pd²⁺ ions (unless otherwise indicated, all ionic forms of Pd are denoted here as Pd²⁺, but it is understood that this includes various complexes of Pd²⁺ with water and Cl⁻). Finally, a 10-fold molar excess of an aqueous 1.0 M NaBH₄ solution was added to the resulting G6-OH(Pd²⁺)₅₅ precursor complex, and reduction was allowed to proceed for 30 min. The final volume of each solution was 10.0 mL.

Characterization. UV–vis absorbance spectra were obtained using a Hewlett-Packard HP8453 spectrometer and a quartz cuvette having an optical path length of 1.00 cm. Depending on the samples, either water (no dendrimer) or a 2.0 μ M (unless otherwise noted) aqueous solution of dendrimer was used for background subtraction.

The acid/base titrations of the dendrimers were carried out using 4.0 mL of 100.0 μ M aqueous solutions of G4-OH, G6-OH, G4-NH₂, and G6-NH₂ dendrimer. The initial pH of the solutions was set using 0.30 NaOH, and the titrant was 0.30 M HCl. A pH 211 Microprocessor pH meter (HANNA instruments, Woonsocket, RI) was used to collect the data.

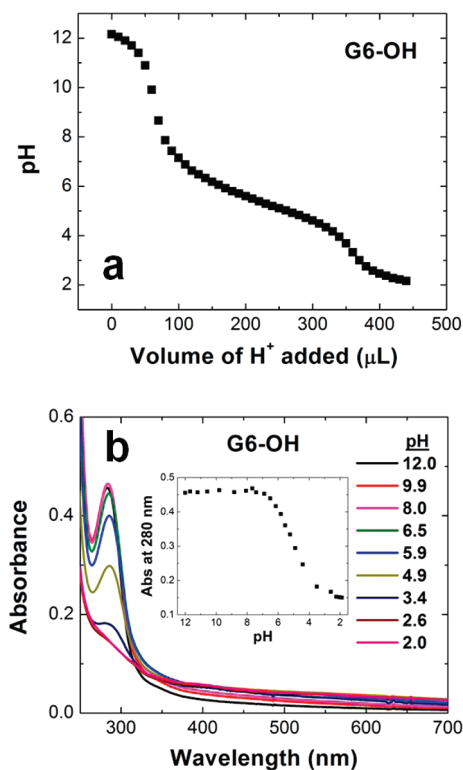


Figure 1. (a) Quantitative acid/base titration of 4.00 mL of a 100.0 μ M G6-OH PAMAM dendrimer solution. (b) Representative absorption spectra of G6-OH as a function of pH. The inset in (b) shows how the band at 280 nm changes as a function of pH. The pH of the initial G6-OH dendrimer solution was 9.0, but it was adjusted to pH 12 with 0.30 M NaOH prior to performing the titrations. The titrant was 0.30 M HCl. All spectra were referenced to water.

RESULTS AND DISCUSSION

Effect of pH on Absorption Spectra. We²⁹ and others^{30,31} have previously reported titration data for PAMAM dendrimers. The results of these studies have shown that the G4-OH dendrimer has one end point,²⁹ while G4-NH₂ and G6-NH₂ exhibit two end points.^{29,30} The pK_a for the interior tertiary amine groups of G4-OH and G4-NH₂ dendrimers is \sim 6.3, and the pK_a for the terminal primary amines of Gn-NH₂ is \sim 9.2.²⁹

Figure 1a is a titration curve for the G6-OH PAMAM dendrimer. The titration began at pH 12.0 and ended at pH 2.0. The data reveal two end points at 60.0 and 360.0 μ L. The equivalents of H⁺ added between these end points corresponds to the number required to fully protonate the interior tertiary amines. A simple calculation shows there are nominally 1.0×10^{-4} equiv of tertiary amine groups present in the initial dendrimer solution, and that these required 0.90×10^{-4} equiv of H⁺ for complete titration. We conclude that, within experimental error, all tertiary amines are protonated at the second end point of the titration.

Figure 1b presents UV–vis spectra of unbuffered, aqueous solutions containing 100.0 μ M G6-OH dendrimers corresponding to the pH range shown in Figure 1a. Between pH 12.0 and pH 3.4, the dendrimer solution exhibits a distinct absorption band with λ_{max} ranging between 280 and 285 nm. Notice that this band nearly disappears at pH \leq 2.6. The inset of Figure 1b is a plot of the uncorrected absorbance at $\lambda_{\text{max}} = 280$ nm as a function of

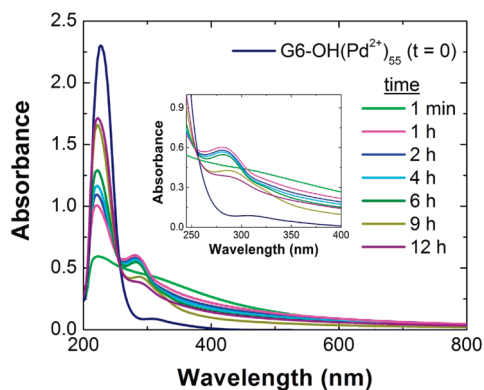


Figure 2. Absorption spectra of a 2.0 μM G6-OH(Pd₅₅) solution as a function of time after reduction of the G6-OH(Pd²⁺)₅₅ precursor complex ($t = 0$) with BH₄⁻. The inset shows an expanded view of the spectral region of interest. All spectra were referenced to a 2.0 μM G6-OH solution. All solutions were exposed to air throughout these experiments.

solution pH. The data in this inset represent the complete set of UV–vis data, while only selected spectra are shown in the main figure. Note that the results shown in the inset are completely reversible. The key finding is that the disappearance of the 280–285 nm absorption band is coincident with complete protonation of the dendrimer.

UV–vis absorption spectra as a function of pH for a G4-OH dendrimer solution, obtained under conditions identical to those described for G6-OH, are provided in the Supporting Information (Figure S1). The results are similar to those obtained for G6-OH. Specifically, an absorption peak is observed in the 280–285 nm range at high pH, but it decreases at lower pHs. Interestingly, however, this band does not completely disappear even at pH 2.0. We also obtained UV–vis absorption spectra for G6-NH₂ and G4-NH₂ dendrimers as a function of pH, and the details are provided in the Supporting Information (Figures S2 and S3, respectively). For G6-NH₂, two indistinct end points are observed, which correspond to sequential protonation of its tertiary and primary amines. The situation for G4-NH₂ is similar to that of G6-NH₂, but it was difficult to obtain fully reproducible results in this case. Full details are provided in the Supporting Information.

Finally, as mentioned in the Introduction, Fu and co-workers have also obtained UV–vis spectra as a function of pH for amine-terminated PAMAM dendrimers.¹⁷ Specifically, they reported that for G1–G4 sectorial PAMAM dendrimers and G2-NH₂, the absorption band at 285 nm decreases with increasing pH. This is exactly the opposite of our findings, and we are not able to offer an explanation for this apparent discrepancy.

UV–vis Spectroscopic Analysis during Synthesis of Pd and Pt DENs. As discussed in the Experimental Section, the synthesis of Pd DENs consists of two steps. First, 55 equiv of Pd²⁺ is mixed with G6-OH, and this results in a precursor complex (G6-OH(Pd²⁺)₅₅) in which Pd²⁺ is bound to the interior tertiary amine groups of the dendrimers.^{1,2} Second, the G6-OH(Pd²⁺)₅₅ precursor complex is reduced with BH₄⁻ to yield zerovalent G6-OH(Pd₅₅) DENs.

Figure 2 shows UV–vis spectra of G6-OH(Pd²⁺)₅₅ as a function of time after addition of the BH₄⁻ reducing agent. Note that the solution was stirred in a vial open to the laboratory atmosphere during these experiments. Prior to reduction ($t = 0$), the UV–vis

absorption spectrum of G6-OH(Pd²⁺)₅₅ displays a strong LMCT band at 224 nm arising from the interaction between Pd²⁺ and the tertiary amines of the dendrimer.^{1,2} However, there is little or no absorbance apparent around 285 nm. Immediately after addition of BH₄⁻ ($t = 1$ min), the LMCT band is replaced by a broad absorption that monotonically increases toward higher energy. This type of spectrum is characteristic of metallic nanoparticles: in this case, G6-OH(Pd₅₅).¹³

At longer times, and in the presence of air, the LMCT peak grows back into the spectrum (its position shifts slightly due to convolution with the baseline), the intensity of the broad feature decreases, and an isosbestic point appears at 250 nm. All of these observations are consistent with a time-dependent, air-induced partial oxidation of G6-OH(Pd₅₅) back to the G6-OH(Pd²⁺)₅₅ precursor complex.¹ In addition to these easily interpretable observations, a new peak at ~ 280 nm is observed after 1 h. This is the same peak observed during the previously described titration experiments.

As discussed earlier, the height of the peak centered at ~ 280 nm decreases upon protonation of the intradendrimer tertiary amines. The results in Figure 2 suggest a similar trend after reaction of the tertiary amines of G6-OH with Pd²⁺. That is, at $t = 0$, the 280 nm band is not apparent in the spectrum of the precursor complex, G6-OH(Pd²⁺)₅₅, even though the pH of the solution is sufficiently high to exhibit the peak in the absence of Pd²⁺ (Figure 1b). However, within 1 h of adding BH₄⁻, the 280 nm peak emerges. We attribute this observation to unblocking of the tertiary amine groups previously complexed to Pd²⁺, which is a necessary consequence of nanoparticle formation. As time progresses, however, this band begins to recede again, until at $t = 12$ h it is nearly gone. This is likely a consequence of re-oxidation of the encapsulated DENs and subsequent recomplexation of Pd²⁺ to the interior amine groups.¹ This latter conclusion is supported by the coincident regrowth of the LMCT band at $\lambda_{\text{max}} = 224$ nm.

In addition to Pd DENs, we also carried out a complete UV–vis analysis of G6-OH(Pt₅₅) DENs to expand the scope of this study. These spectroscopic experiments were performed similarly to those described for Pd. A detailed analysis of the results is provided in the Supporting Information, but they are briefly summarized here. Prior to reduction, the UV–vis spectrum of G6-OH(Pt²⁺)₅₅ reveals two bands.³² A very small peak at $\lambda_{\text{max}} = 215$ nm arises from Pt²⁺ in solution,³³ and a more intense LMCT peak at $\lambda_{\text{max}} = 250$ nm is due to the interaction between Pt²⁺ and the tertiary amines of the dendrimer.^{34–36} After addition of BH₄⁻, however, spectra of the resulting Pt DENs are quite different than those of the Pd DENs shown in Figure 2. Specifically, the peak at 280 nm is very small or absent. On the basis of our previous studies of Pt DENs, this observation is easily explained. First, we recently showed that the reduction of the G6-OH(Pt²⁺)_n precursor is much slower than it is for the Pd analogue.^{1,32} Hence, even after 12 h (the maximum time represented in Figure S5), the precursor is only partially reduced. Second, the synthesis of Pt DENs results in a bimodal distribution of fully reduced DENs and unreduced G6-OH(Pt²⁺)_n precursor.³² Indeed, when the synthesis is performed using a 55:1 ratio of Pt²⁺:G6-OH, only $\sim 14\%$ of the precursor complex is reduced to G6-OH(Pt₅₅).³² For these two reasons, only a small percentage of the tertiary amines are unblocked after addition of BH₄⁻, and hence the band at 280–285 nm is not observed.

Effect of Purification by Centrifugation. Figure 3 shows UV–vis spectra before and after filtration of a 100.0 μM , pH 9.0

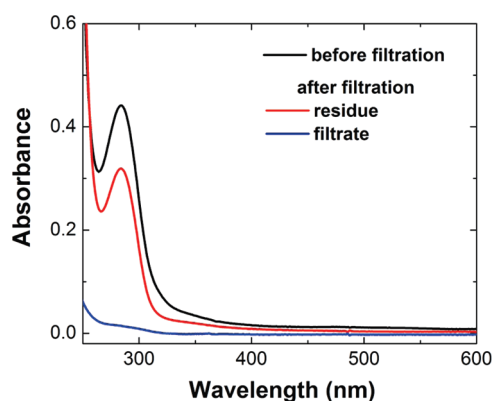


Figure 3. Absorption spectra obtained from an aqueous G6-OH dendrimer solution before and after filtration through a spin filter having a nominal molecular weight limit (NMWL) of 10.0 kDa. The centrifugation rate and time were 5000 g (ms^{-2}) and 30.0 min, respectively. Before filtration, the G6-OH concentration was 100.0 μM . All spectra were referenced to water.

aqueous solution of G6-OH using a spin filter having a nominal molecular weight limit (NMWL) of 10.0 kDa. The nominal molecular weight of the G6-OH dendrimer is 58.0 kDa. Before centrifugation, the band associated with the tertiary amines of the dendrimer is present at $\lambda_{max} = 280$ nm. After centrifugation, the residue retained by the filter was taken up in water, and the same peak was found to be present in the spectrum. The intensity of this peak is a little lower than it was before centrifugation, but this is just a consequence of imperfect recovery of the dendrimer from the filter. Importantly, the spectrum of the centrifugate reveals almost no absorbance in the 280–285 nm range. Taken together, these results show that the absorbance observed prior to filtration arises exclusively from intact, or nearly intact, dendrimers rather than fragments having molecular weights below the 10.0 kDa cutoff of the filter. Results consistent with those just described for G6-OH were also found for G4-OH (Supporting Information, Figure S6).

Analysis of a Model Compound. To confirm that the absorption band in the 280–285 nm range arises from naked tertiary amines of the dendrimer, we examined the UV–vis spectrum of a model compound. The model compound, 1-[bis-[3-(dimethylamino)-propyl]amino]-2-propanol (inset, Figure 4a), contains three tertiary amines and one primary hydroxyl group. Like the PAMAM dendrimers, the primary hydroxyl group is attached to a tertiary amine.

Figure 4a presents a quantitative titration of the model compound starting at pH 11.4, which is the pH of an aqueous 10.0 mM solution, and ending at pH 2.0. The titration curve reveals two end points, which likely correspond to protonation of the tertiary amine groups. Figure 4b shows UV–vis spectra corresponding to the titration curve in Figure 4a. The model compound exhibits an absorption band at 280–285 nm between pH 11.4 and 7.7. Little change in the absorption spectrum is observed below pH 7.7. The inset of Figure 4b is a plot of the uncorrected absorbance at 280 nm, and it clearly reveals the relationship between protonation of the tertiary amines in the model compound and the absorbance at 280 nm. As for the dendrimers, the pH-dependent behavior of the model compound is fully reversible. The important point is that the model compound, which is structurally similar to part of a dendrimer branch, exhibits similar spectroscopic behavior. Hence, its characteristics

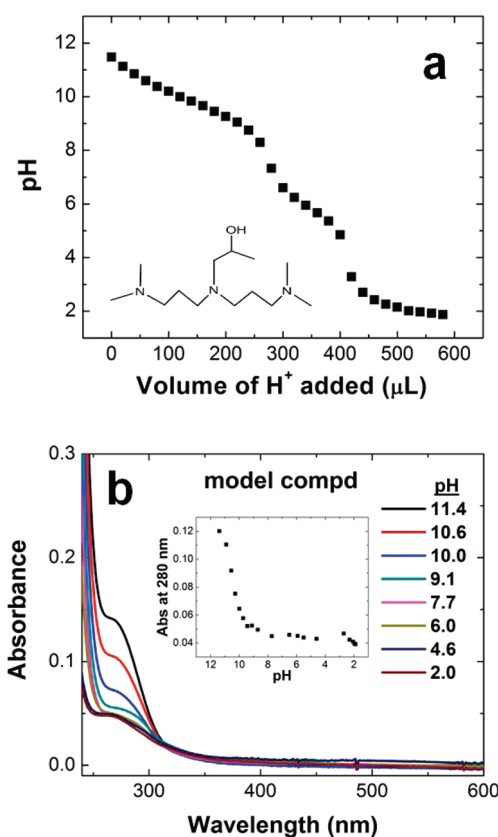


Figure 4. (a) Quantitative acid/base titration of the model compound shown in the inset. (b) Absorption spectra of the model compound as a function of pH. The inset shows how the absorbance at 280 nm changes as a function of pH. In all cases, the concentration of the model compound was 10.0 mM, which results in an initial pH of 11.4. The titrant was 0.30 M HCl, and the titrated volume was 4.0 mL. All spectra were referenced to water.

further reinforce our interpretation of the origin of the band at ~ 280 nm.

SUMMARY AND CONCLUSIONS

In summary, we have reported a UV–vis spectroscopic study of PAMAM dendrimers as a function of pH. We find that the degree of protonation of the interior tertiary amines of four different PAMAM dendrimers correlates directly to an absorption band in the range of 280–285 nm. Specifically, at low pH, the tertiary amines are protonated, and the 280–285 nm band is absent. However, at elevated pH, when these groups are deprotonated, this band appears. Similar results were obtained for a simple model compound. The dependence of the 280–285 nm band on the chemical state of the tertiary amines of the dendrimers was confirmed by complexing them with Pd^{2+} and Pt^{2+} . In this case the band disappears, and it only reappears when the metal ions are decomplexed following reduction with BH_4^- . Finally, filtration experiments showed that the absorption band between 280 and 285 nm arises exclusively from intact, or nearly intact, dendrimers rather than low-molecular-weight fragments.

The results reported in this Article are important for studies involving the synthesis of metal nanoparticles, or other objects, within the dendrimer interior. This is because the peak between

280–285 nm interferes strongly with other characteristic bands in this region. However, it can be rendered silent simply by lowering the pH of the dendrimer solution.

ASSOCIATED CONTENT

S Supporting Information. Quantitative acid/base titrations and pH-dependent spectroscopic studies of G4-OH, G6-NH₂, and G4-NH₂ PAMAM dendrimers, a time-dependent UV–vis study of Pt DENs, and absorption spectra of a G4-OH dendrimer solution before and after centrifugation. This material is available free of charge via the Internet at <http://pubs.acs.org>.

AUTHOR INFORMATION

Corresponding Author

*E-mail: crooks@cm.utexas.edu.

ACKNOWLEDGMENT

We gratefully acknowledge the National Science Foundation (Grant No. 0847957) for financial support of this work. We also acknowledge the Robert A. Welch Foundation (Grant No. F-0032) for sustained support of our research program. Finally, we thank Dr. Javier Guerra for valuable discussions.

REFERENCES

- (1) Carino, E. V.; Knecht, M. R.; Crooks, R. M. *Langmuir* **2009**, *25*, 10279–10284.
- (2) Scott, R. W. J.; Ye, H.; Henriquez, R. R.; Crooks, R. M. *Chem. Mater.* **2003**, *15*, 3873–3878.
- (3) Crooks, R. M.; Zhao, M.; Sun, L.; Chechik, V.; Yeung, L. K. *Acc. Chem. Res.* **2000**, *34*, 181–190.
- (4) Kim, Y.-G.; Oh, S.-K.; Crooks, R. M. *Chem. Mater.* **2003**, *16*, 167–172.
- (5) Scott, R. W. J.; Wilson, O. M.; Crooks, R. M. *J. Phys. Chem. B* **2005**, *109*, 692–704.
- (6) Albiter, M. A.; Crooks, R. M.; Zaera, F. J. *Phys. Chem. Lett.* **2010**, *1*, 38–40.
- (7) Ozturk, O.; Black, T. J.; Perrine, K.; Pizzolato, K.; Williams, C. T.; Parsons, F. W.; Ratliff, J. S.; Gao, J.; Murphy, C. J.; Xie, H.; Ploehn, H. J.; Chen, D. A. *Langmuir* **2005**, *21*, 3998–4006.
- (8) Huang, W.; Kuhn, J. N.; Tsung, C.-K.; Zhang, Y.; Habas, S. E.; Yang, P.; Somorjai, G. A. *Nano Lett.* **2008**, *8*, 2027–2034.
- (9) Lang, H.; Maldonado, S.; Stevenson, K. J.; Chandler, B. D. *J. Am. Chem. Soc.* **2004**, *126*, 12949–12956.
- (10) Peng, X.; Pan, Q.; Rempel, G. L.; Wu, S. *Catal. Commun.* **2009**, *11*, 62–66.
- (11) Gates, A. T.; Nettleton, E. G.; Myers, V. S.; Crooks, R. M. *Langmuir* **2010**, *26*, 12994–12999.
- (12) Knecht, M. R.; Garcia-Martinez, J. C.; Crooks, R. M. *Langmuir* **2005**, *21*, 11981–11986.
- (13) Creighton, J. A.; Eadon, D. G. *J. Chem. Soc., Faraday Trans.* **1991**, *87*, 3881–3891.
- (14) Esumi, K.; Suzuki, A.; Aihara, N.; Usui, K.; Torigoe, K. *Langmuir* **1998**, *14*, 3157–3159.
- (15) Garcia, M. E.; Baker, L. A.; Crooks, R. M. *Anal. Chem.* **1999**, *71*, 256–258.
- (16) Zheng, J.; Petty, J. T.; Dickson, R. M. *J. Am. Chem. Soc.* **2003**, *125*, 7780–7781.
- (17) Wang, Y.; Niu, S.; Zhang, Z.; Xie, Y.; Yuan, C.; Wang, H.; Fu, D. *J. Nanosci. Nanotechnol.* **2010**, *10*, 4227–4233.
- (18) Lee, W. I.; Bae, Y.; Bard, A. J. *J. Am. Chem. Soc.* **2004**, *126*, 8358–8359.
- (19) Maiti, P. K.; Çagin, T.; Lin, S.-T.; Goddard, W. A. *Macromolecules* **2005**, *38*, 979–991.
- (20) Maiti, P. K.; Çagin, T.; Wang, G.; Goddard, W. A. *Macromolecules* **2004**, *37*, 6236–6254.
- (21) Gomez, M. V.; Guerra, J.; Velders, A. H.; Crooks, R. M. *J. Am. Chem. Soc.* **2009**, *131*, 341–350.
- (22) Zhou, L.; Russell, D. H.; Zhao, M.; Crooks, R. M. *Macromolecules* **2001**, *34*, 3567–3573.
- (23) Shi, X.; Bányai, I.; Islam, M. T.; Lesniak, W.; Davis, D. Z., Jr.; Baker, J. R.; Balogh, L. P. *Polymer* **2005**, *46*, 3022–3034.
- (24) Cason, C. A.; Oehrle, S. A.; Fabré, T. A.; Girten, C. D.; Walters, K. A.; Tomalia, D. A.; Haik, K. L.; Bullen, H. A. *J. Nanomater.* **2008**, 1–7.
- (25) Islam, M. T.; Shi, X.; Balogh, L., Jr.; Baker, J. R. *Anal. Chem.* **2005**, *77*, 2063–2070.
- (26) Wales, C. H.; Berger, J.; Blass, S.; Crooks, R. M.; Asherie, N. *Langmuir* **2011**, *27*, 4104–4109.
- (27) Liu, Y.; Bryantsev, V. S.; Diallo, M. S.; Goddard, W. A., III. *J. Am. Chem. Soc.* **2009**, *131*, 2798–2799.
- (28) Tomalia, D. A.; Naylor, A. M.; Goddard, W. A. *Angew. Chem., Int. Ed. Engl.* **1990**, *29*, 138–175.
- (29) Niu, Y.; Sun, L.; Crooks, R. M. *Macromolecules* **2003**, *36*, 5725–5731.
- (30) Cakara, D.; Kleimann, J.; Borkovec, M. *Macromolecules* **2003**, *36*, 4201–4207.
- (31) Tomalia, D. A.; Baker, H.; Dewald, J.; Hall, M.; Kallos, G.; Martin, S.; Roeck, J.; Ryder, J.; Smith, P. *Polym. J.* **1985**, *17*, 117–132.
- (32) Knecht, M. R.; Weir, M. G.; Myers, V. S.; Pyrz, W. D.; Ye, H.; Petkov, V.; Buttrey, D. J.; Frenkel, A. I.; Crooks, R. M. *Chem. Mater.* **2008**, *20*, 5218–5228.
- (33) Elding, L. I.; Olsson, L. F. *J. Phys. Chem.* **1978**, *82*, 69–74.
- (34) Ye, H.; Scott, R. W. J.; Crooks, R. M. *Langmuir* **2004**, *20*, 2915–2920.
- (35) Zhao, M.; Crooks, R. M. *Angew. Chem., Int. Ed.* **1999**, *38*, 364–366.
- (36) Fanizzi, F. P.; Intini, F. P.; Maresca, L.; Natile, G. *J. Chem. Soc., Dalton Trans.* **1990**, 199–202.